Thermal Science and Engineering Progress 40 (2023) 101797

Contents lists available at ScienceDirect

Thermal Science and Engineering Progress

journal homepage: www.sciencedirect.com/journal/thermal-science-and-engineering-progress

Effects of combined radiation and forced convection on a directly capturing solar energy system

Oguzhan Kazaz [a], Nader Karimi [a,b], Shanmugam Kumar [a], Gioia Falcone [a], Manosh C. Paul [a,*]

[a] Systems, Power & Energy Research Division, James Watt School of Engineering, University of Glasgow, Glasgow G12 8QQ, UK
[b] School of Engineering and Materials Science, Queen Mary University of London, London E1 4NS, UK

ARTICLE INFO

Keywords:
Solar radiation
Nanofluids
Volumetrically heated
Thermal performance
Photo-thermal conversion
Numerical simulation

ABSTRACT

In this study, the photo-thermal conversion performance of volumetrically heated solar collector with mono-nanoparticle and hybrid-nanoparticle filled fluids desired for a direct solar energy system is numerically investigated. Considering the scattering and absorption characteristics of the heat transfer fluid in the translucent medium, its thermal performance in the collector is analysed solving the radiative transport, energy, and Navier-Stokes equations. A systematic parametric study is conducted by selectively changing the fluid type, volume concentration nanoparticle, operating temperature, and collector length to evaluate their influence on the thermal capacity of the collector. The results reveal that the use of nanoparticles and the increase in volume concentration improves the solar energy absorption capacity of the heat transfer nanofluids, thus increasing the photo-thermal conversion performance. Besides, it is found that the increase in the fluid inlet temperature increases the heat losses, resulting in a decrease in the amount of usable heat generated from solar energy. Furthermore, although the heat gain and useful heat generation of the fluid increase as the collector length increases, the thermal performance of the collector decreases due to increasing heat losses. Moreover, it is shown that the performance evaluation criterion (PEC) of water-based Graphite, TiO_2 and Ag mono nanofluids is 1.6, 1.56, and 1.43, respectively while water-based Graphite + MgO, TiO_2 + MgO and Ag + MgO blended nanofluids is 1.68, 1.66, and 1.58, respectively. Because the blended nanoparticles increase the solar energy absorption capacity, both the thermal performance of the collector and the sensible energy storage capacity are enhanced. The findings of the study suggest that hybrid nanofluids can be considered as an effective heat transfer fluid that can be used in solar energy applications.

Introduction

Increasing energy demands cause both an increase in the use of fossil fuels and costs [1,2]. However, due to the limited reserve of fossil fuels and their harm to the environment such as greenhouse emissions, the importance of researching and utilizing energy sources that can be alternatives to the traditional fuels has emerged [3,4]. Therefore, such non-traditional energy sources, known as renewable energy, is increasing in use because of its various advantages such as sustainability, environmental friendliness, easy availability and generatability, contributing to the economic growth [5,6].

Among various renewable energy sources, solar energy has an important position as a heat and electricity source. In order to benefit from these advantages of solar energy, first of all, it needs to be collected. For this, it is necessary to use solar collectors that can convert solar radiation into thermal energy. In conventional solar collectors, where the solar energy is first absorbed by the absorber surface and transferred to the heat transfer fluid, the efficiency of the collector decreases owing to the heat losses due to the high temperature difference between the heat transfer fluid and the absorber plate [7]. The direct absorption of solar radiation by the heat transfer fluid, however, offers the opportunity to minimize the heat losses. In these systems, which are called direct absorption solar collectors, the heat transfer fluid can improve the thermal performance of the collector since it acts as both an absorbing medium and a working fluid [8].

The heat transfer fluid in closed media can move in the cavity with the effect of natural convection due to the temperature difference. In media where solar energy is directly absorbed by the heat transfer fluid, besides natural convection, radiation also has an effect. Hence, the absorption capacity of the working fluid is important in direct absorption systems where the combined effect of radiation and free convection is

* Corresponding author.
E-mail address: Manosh.Paul@glasgow.ac.uk (M.C. Paul).

https://doi.org/10.1016/j.tsep.2023.101797
Received 21 October 2022; Received in revised form 19 February 2023; Accepted 10 March 2023
Available online 16 March 2023

Nomenclature

L	Length of the collector (m)
H	Height of the collector (m)
AR	Aspect ratio
I_λ	Radiation intensity (W/m^{2}μm)
$\vec{r}$	Position vector
$\vec{s}$	Direction vector
$I_{b\lambda}$	Black body intensity (W/m^{2}μm)
n	Refractive index
$\vec{s}'$	Scattering direction vector
σ_s	Scattering coefficient (1/m)
α_λ	Spectral absorption coefficient (1/m)
k	Absorption index
n	Refractive index
f_v	Particle volume concentration
$Q_{e\lambda}$	Extinction efficiency
D	Diameter of the particle (m)
m	Normalized refractive index of the particle to the fluid
α	Size parameter
$Q_{a\lambda}$	Absorption efficiency
$Q_{s\lambda}$	Scattering efficiency
$K_{e\lambda}$	Extinction coefficient (1/m)
$K_{a\lambda}$	Absorption coefficient (1/m)
$K_{s\lambda}$	Scattering coefficient (1/m)
C_p	Specific heat (J/kgK)
K	Thermal conductivity (W/mK)
h	Convective heat transfer coefficient
ε	Dielectric constant
r	Radius of the nanoparticle
u, v	Velocity vectors (m/s)
p	Pressure (Pa)
G	Gravitational acceleration (m/s^2)
T	Temperature (K)
V	Velocity of the working fluid (m/s),
q	Heat flux (W/m^2)
D_h	Hydraulic diameter (m)
L	Length (m)
G	Solar intensity (W/m^2)
ΔP	Pressure loss (Pa)
ΔH	Enthalpy change (J/kg)
$\dot{m}$	Mass flow rate (kg/s)
$\dot{Q}_s$	Rate of stored energy (W)
Q	Rate of useful heat (W)
PEC	Performance evaluation criterion
H	Total heat loss (W/m^2)

Greek symbols

ρ	Density (kg/m^3)
μ	Dynamic viscosity (Ns/m^2)
Φ	Dissipation functions
σ	Stefan-Boltzmann(5.67×10^{-8} W/m^{2}K^4)
ε	Emissivity
φ	Nanoparticle concentration
λ	Wavelength of incident light (μm)
Φ	Phase function
Ω'	Solid angle
ρ	Density (kg/m^3)
k_B	Boltzmann constant (1.3807×10^{-23} J/K)

Subscripts

nf	Nanofluid
p	Nanoparticle
f	Base fluid
amb	Ambient
hnf	Hybrid nanofluid
eff	Effective
*s*1	First nanoparticle
*s*2	Second nanoparticle
s	Stored
h	Hot
c	Cold
conv	Convective
rad	Radiative
in	Inlet
out	Outlet

observed. Therefore, the addition of nanoparticles to pure fluids can improve the thermal performance of the cavity as well as the capacity of the fluid to absorb solar energy [9,10,11,12,13,14,15]. Hatami and Jing [14] numerically examined the thermal capacity of the solar collector with different nanoparticle types that are TiO_2, Al_2O_3 and CuO via finite element analysis. As different wall types and boundary conditions were used, the mean and local Nusselt numbers were calculated. The results revealed that the collector with wavy bottom wall had the maximum Nusselt number compared to that of flat collector. In addition, water based TiO_2 nanofluid had the highest Nusselt number. Absorption capacities of Ag, ZnO and TiO_2 nanoparticles were analysed by Chen *et al.* [15] by performing experiments. They found that Ag nanoparticles had better thermal efficiency at low/very low particle concentrations, and it increased with increasing nanoparticle concentration. The photo-thermal conversion efficiency of water-based Ag nanofluid was 84.61% after 5 min of radiation.

Because the fluid velocity can affect the thermal performance of the collector, on the other hand, flow conditions can be considered as another parameter affecting the photothermal conversion performance of the direct absorption solar collectors [16,17,18,19]. Gorji and Ranjbar [18] experimentally investigated the effects of nanoparticle concentration, solar flux, and flow rate on solar-thermal capacity. The results showed that water-based magnetite nanofluids had better exergy and thermal efficiencies compared to the graphite and silver nanofluids. It was also found that the thermal efficiency decreased despite enhanced exergy efficiency with increasing solar flux. It was further seen that increasing the nanoparticle concentration by more than 25–30 ppm did not cause any significant improvements in the thermal and exergy efficiencies. Luo *et al.* [19] both experimentally and numerically analysed the thermal performance of oil based TiO_2, Al_2O_3, Ag, Cu, SiO_2, graphite nanoparticles, and carbon nanotubes. The results indicated that the photo-thermal conversion efficiencies were 122.7% and 117.5% for nanofluids with 0.01 vol% graphite and 0.5 vol% Al_2O_3, respectively. It was found that the nanoparticles improved the exit temperature and efficiency by 30–100 K and 2–25%, respectively, compared to the base oil.

Type of fluid used in solar energy systems are the most important elements that affect the efficiency of heat transfer. As a result, investigation of the effect of hybrid nanoparticles in the fluid on the thermal performance in different types of solar collectors has been carried out in recent years [20,21,22,23]. Hybrid nanoparticles not only have the potential to improve the thermal properties of the working fluid, but they can also improve fluid's absorption capacity in direct absorption systems. The effects of SiO_2/Ag and CuO nanoparticles on thermo-physical and optical properties and photo-thermal conversion efficiency were explored by Joseph *et al.* [24] via experiments in a motionless

direct absorption solar collector. It was found that solar radiation capacity of SiO_2/Ag nanoparticles-based fluids increased with the addition of CuO nanoparticles. It was further observed that the optical and thermal properties altered by the surfactant's fraction, and the thermal efficiency improved due to the absorbance capacity of nanoparticles. Furthermore, an experimental study on direct absorption solar collector for the investigation of entropy and exergy was performed by Karami [25] with blended nanoparticles of Fe_3O_4/SiO_2 dispersed in water. Different nanofluid concentrations (e.g. 500 ppm, 1000 ppm, and 2000 ppm), and different flow rates (e.g 0.0075, 0.0.015, and 0.0225 kg/s) were used. The results demonstrated that the efficiency enhanced with the increase of both the particle concentration and flow rate. When the volume concertation increased from 0 to 2000 ppm, it was observed that the augmentation of exergy efficiency increased to 66.4% at a mass flow rate of 0.0225 kg/s.

As per the literature review, although, that the thermal energy is generated by using single nanoparticles in most of the studies, detailed understanding of the use of blended nanoparticles in the application of direct absorption solar systems is still missing. Because hybrid nanoparticles are a combination of different types of particles, their thermophysical and optical properties are different from those of their constituents. As a result, their effects on the thermal performance of the collector may be different. Besides, although the thermal conversion performance of nanofluids under static conditions has been widely explored, the influence of the flow velocity, the collector geometry and working conditions on solar energy absorption characteristics of nanofluids is not yet fully understood. Changing the concentration of nanoparticles means a change in the flow rate, since the thermophysical properties of the nanofluid change. So, an increase or decrease of the flow rate could also affect the heating time of the nanofluid by the solar energy and consequently, the flow time in the collector – the effect of which in combination with the flow velocity needs to be investigated.

Additionally, nanoparticle volume concentration is a factor that directly affects both the thermophysical and optical properties of the heat transfer fluid. The capacity of the volumetrically heated nanofluid to capture solar energy further depends on the volume concentration. Therefore, high concentration is favourable to increase the efficiency of photo-thermal transformation that takes place at low concentrations. However, to what extent or how the effect of this high concentration can affect the thermal performance of the collect is still fully addressed. This also poses further challenges on the overall system performance, when this is combined with the effects of collector geometry and operating temperature of hybrid nanoparticles. Finally, the combined effect of direct heating, radiation, forced convection and heat losses in volumetric solar collectors is still unknown when a translucent medium absorbs, emits, or scatters radiation. In this case, the irradiation power cannot remain constant [26], so the heat transfer and flow properties of the fluid in the collector continuously change. Therefore, further research is required to examine the influence of this combined effect on the thermal performance of hybrid particles incorporated nanofluids. Consequently, the main aim of the current study is to investigate the photo-thermal conversion performances of volumetrically heated nanofluids by filling the specified knowledge gaps.

Problem statement and mathematical modelling

A 2D volumetric solar collector in which solar radiation passes vertically through nanoparticle filled heat transfer fluid, as shown in Fig. 1(a). The top surface is surrounded by a highly transparent glass plate to facilitate absorption of radiation by the working fluid, and there is also a combined radiation and convection heat loss from the glass to the atmosphere. The process of capturing radiation is illustrated in Fig. 1 (b) [27], and the nanoparticles with increasing energy start to augment the temperature of the nanofluid by colliding with each other. Extant works indicate that the aspect ratio (L/H) of the cavity is about 10 [28].

The Radiative Transfer Equation (RTE) is applied to assess the spectral attenuation of radiation within the semi-translucent medium, and it can be expressed as [29]:

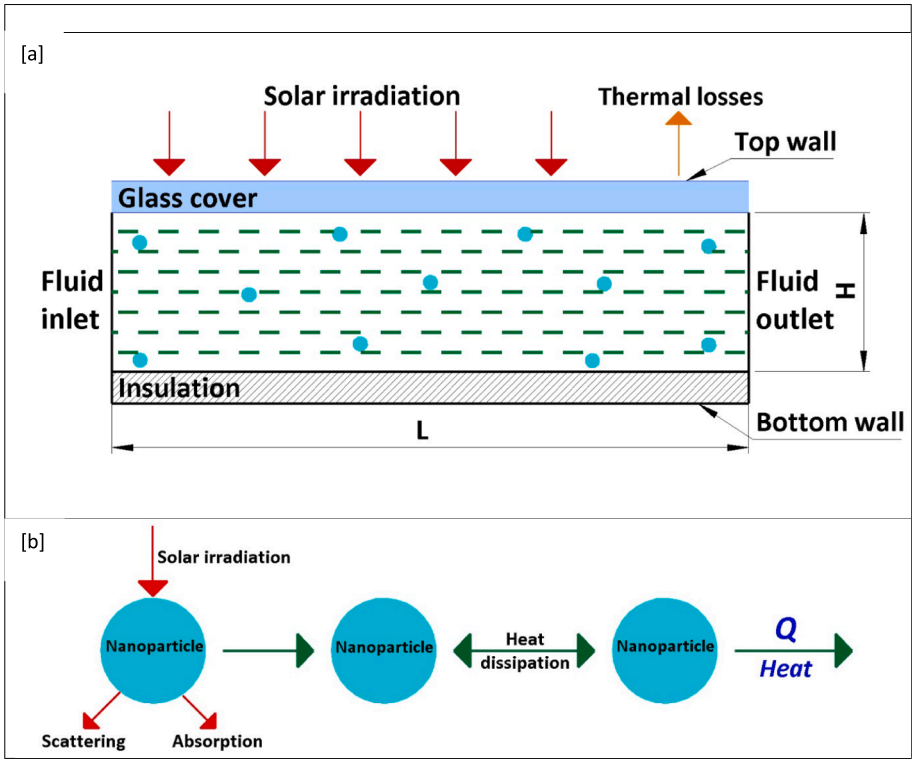

Fig. 1. (a) A 2D schematic of a volumetric collector, (b) Impact and action of radiation on a nanoparticle inside the heat transfer fluid.

$$\nabla \bullet (I_\lambda(\vec{r},\vec{s})\vec{s}) + (\alpha_\lambda+\sigma_s)I_\lambda(\vec{r},\vec{s}) = \alpha_\lambda n^2 I_{b\lambda} + \frac{\sigma_s}{4\pi}\int_0^{4\pi} I_\lambda(\vec{r},\vec{s}')\Phi(\vec{s}\bullet\vec{s}')d\Omega' \quad (1)$$

where I_λ is the radiation intensity, $\vec{r}$ is the position vector, $\vec{s}$ is the direction vector, α_λ is the spectral absorption co-efficient,σ_s is the scattering co-efficient, $I_{b\lambda}$ is the black body radiation intensity, $\vec{s}'$ is the scattering direction vector, n is the refractive index, Φ is the phase function and Ω' is the solid angle.

Scattering effects of the host fluid can be ignored since the absorption dominates the attenuation in pure fluids so that the extinction coefficient can be described as [30]:

$$K_{e\lambda,bf} = K_{a\lambda,bf} = \frac{4\pi k}{\lambda} \quad (2)$$

Nanoparticles, however, affect attenuation due to both scattering and absorption properties. Therefore, some factors such as particle concentration can affect the semi-translucent medium. The Rayleigh scattering can be used for small particles in order to calculate the optical properties of nanofluids [31,32].

The extinction coefficient can be described as [30]:

$$K_{e\lambda,np} = \frac{3f_v Q_{e\lambda}(a,m)}{D} \quad (3)$$

where f_v is the nanoparticle concentration, $Q_{e\lambda}$ is the extinction efficiency,D is the particle size,α is the size parameter, and m is the normalized refractive index of the particle to the fluid. m and α can be given as [30]:

$$m = \frac{m_{particles}}{n_{fluid}} \quad (4)$$

$$m_{particles} = n + ik \quad (5)$$

$$\alpha = \frac{\pi D}{\lambda} \quad (6)$$

where k and n are the absorption and refractive indexes of the nanoparticle, respectively. The optical and dielectric constants of the nanoparticle and water is taken from literature [33,34,35]. In addition, if the dielectric constant, ε, of nanoparticle is known, it can be converted into absorption and refractive indexes using Eqs. (7) and (8) [32]:

$$n = \left(\frac{\left(\varepsilon_1^2+\varepsilon_2^2+\varepsilon_1\right)^{1/2}}{2}\right)^{1/2} \quad (7)$$

$$k = \left(\frac{\left(\varepsilon_1^2+\varepsilon_2^2-\varepsilon_1\right)^{1/2}}{2}\right)^{1/2} \quad (8)$$

The extinction efficiency is given by [32]:

$$Q_{e\lambda} = Q_{a\lambda} + Q_{s\lambda} \quad (9)$$

where $Q_{a\lambda}$ and $Q_{s\lambda}$ are the absorption efficiency and scattering efficiency, respectively.

$$Q_{a\lambda} = 4\alpha Im\left\{\frac{m^2-1}{m^2+2}\left[1+\frac{\alpha^2}{15}\left(\frac{m^2-1}{m^2+2}\right)\frac{m^4+27m^2+38}{2m^2+3}\right]\right\} \quad (10)$$

$$Q_{s\lambda} = \frac{8}{3}\alpha^4\left|\left(\frac{m^2-1}{m^2+2}\right)\right|^2 \quad (11)$$

Using Eqs. (6) and (9) in Equation (3), the extinction coefficient, $K_{e\lambda}$, can be re-written as:

$$K_{e\lambda} = K_{a\lambda} + K_{s\lambda} \quad (12)$$

where $K_{a\lambda}$ and $K_{s\lambda}$ are the absorption and scattering coefficients, respectively. Note that:

$$K_{a\lambda} = \frac{12\pi f_v}{\lambda} Im\left\{\frac{m^2-1}{m^2+2}\left[1+\frac{\pi^2D^2}{15\lambda^2}\left(\frac{m^2-1}{m^2+2}\right)\frac{m^4+27m^2+38}{2m^2+3}\right]\right\} \quad (13)$$

and

$$K_{s\lambda} = \frac{8\pi^4D^3f_v}{\lambda^4}\left|\left(\frac{m^2-1}{m^2+2}\right)\right|^2 \quad (14)$$

The total extinction coefficient of the nanofluid is the sum of the extinction coefficients of host fluid and nanoparticle:

$$K_{e\lambda,nf} = K_{e\lambda,np} + K_{e\lambda,bf} \quad (15)$$

The total extinction coefficient of hybrid nanofluid is also equal to the sum of the extinction coefficient of each nanoparticle, and host fluid [36]:

$$K_{e\lambda,hybridnf} = K_{e\lambda,bf} + K_{e\lambda,np1} + K_{e\lambda,np2} \quad (16)$$

Since water is considered as a semi-transparent medium in the wavelength range of 200–1200 nm, when the wavelength shifts to the near-infrared region, water becomes an efficient absorber [37]. Therefore, the addition of nanoparticle increases the absorption to a greater extent in this wavelength range, and 85% of the solar energy can reach the earth's surface in this wavelength range [38].

The nanofluid is assumed to be single-phase, incompressible, laminar, and Newtonian. The governing and energy equations are given as:

(i) Continuity equation:

$$\frac{\partial u}{\partial x} + \frac{\partial v}{\partial y} = 0 \quad (17)$$

(ii) x-momentum equation:

$$u\frac{\partial u}{\partial x} + v\frac{\partial u}{\partial y} = -\frac{1}{\rho_{nf}}\frac{\partial p}{\partial x} + \frac{\mu_{nf}}{\rho_{nf}}\left(\frac{\partial^2 u}{\partial x^2} + \frac{\partial^2 u}{\partial y^2}\right) \quad (18)$$

(iii) y-momentum equation:

$$u\frac{\partial v}{\partial x} + v\frac{\partial v}{\partial y} = -\frac{1}{\rho_{nf}}\frac{\partial p}{\partial y} + \frac{\mu_{nf}}{\rho_{nf}}\left(\frac{\partial^2 v}{\partial x^2} + \frac{\partial^2 v}{\partial y^2}\right) \quad (19)$$

(iv) Energy conservation equation:

$$\rho_{nf}c_{p_{nf}}\left(u\frac{\partial T}{\partial x} + v\frac{\partial T}{\partial y}\right) = k_{nf}\left(\frac{\partial^2 T}{\partial x^2} + \frac{\partial^2 T}{\partial y^2}\right) - \frac{\partial q_r}{\partial y} \quad (20)$$

Furthermore, the boundary conditions are:
At the inlet:

$$u = U_{in}, T = T_{in}, v = 0 \quad (21)$$

At the outlet:

$$p = 0 \quad (22)$$

At the top surface:

$$q = h(T - T_{amb}) + \varepsilon\sigma(T^4 - T_{amb}^4) \quad (23)$$

At the bottom:

$$\frac{\partial T}{\partial y} = 0 \quad (24)$$

At the walls' surface:

$$u = v = 0 \quad (25)$$

where h is the convective heat transfer coefficient, σ is the Stefan-Boltzmann constant, $5.67 \times 10^{-8} W/m^2 \bullet K^4$, and T_{amb} is the ambient temperature. The convection heat transfer coefficient, h, is calculated using Duffie correlation as a function of wind speed [39]:

$$h = 5.7 + 3.8v \tag{26}$$

The density, and specific heat of the nanofluid are described by [40]:

$$\rho_{nf} = \rho_f(1-\varphi) + \rho_p\varphi \tag{27}$$

$$(\rho C_p)_{nf} = (\rho C_p)_f(1-\varphi) + (\rho C_p)_p\varphi \tag{28}$$

The density, specific heat, and thermal conductivity of the hybrid nanofluid are described as [41]:

$$\rho_{hnf} = \varphi_{np1}\rho_{np1} + \varphi_{np2}\rho_{np2} + (1-\varphi)\rho_f \tag{29}$$

where,

$$\varphi = \varphi_{np1} + \varphi_{np2} \tag{30}$$

$$(\rho C_p)_{hnf} = \varphi_{np1}\rho_{np1}C_{p,np1} + \varphi_{np2}\rho_{np2}C_{p,np2} + (1-\varphi)\rho_f C_{p,f} \tag{31}$$

$$k_{eff} = k_{static} + k_{Brownian} \tag{32}$$

The static thermal conductivity of nanofluid is described as [42]:

$$k_{static} = k_f\frac{k_p + 2k_f - 2\varphi(k_f - k_p)}{k_p + 2k_f + \varphi(k_f - k_p)} \tag{33}$$

where k_p and k_f are the thermal conductivities of the nanoparticle and base fluid, respectively.

The static thermal conductivity of the hybrid nanofluid can be expressed as [43]:

$$(k_{hnf})_{static} = k_{bf}\frac{k_{s2} + 2k_{bf} - 2\varphi_2(k_{bf} - k_{s2})}{k_{s2} + 2k_{bf} + \varphi_2(k_{bf} - k_{s2})} \tag{34}$$

where,

$$k_{bf} = k_f\frac{k_{s1} + 2k_f - 2\varphi_1(k_f - k_{s1})}{k_{s1} + 2k_f + \varphi_1(k_f - k_{s1})} \tag{35}$$

where, k_{bf} and k_f are the thermal conductivities of the first nanofluid and base fluid. k_{s1} and k_{s2} also represent the thermal conductivities of first and second nanoparticles, respectively. φ_1 and φ_2 represent the particle concentrations.

The effect of Brownian motion on thermal conductivity is given as [44]:

$$k_{Brownian} = \frac{\rho_{np}\varphi C_{p,np}}{2}\sqrt{\frac{k_B T}{3\pi r\mu_{bf}}} \tag{36}$$

where k_B is the Boltzmann constant, $1.3807 \times 10^{-23} J/K$, r is the radius of the nanoparticle, μ_{bf} is the viscosity of the host fluid, and T is the temperature.

The effective viscosity of the nanofluid is described as [45]:

$$\mu_{nf} = \mu_{bf}\left(1 + 39.11\varphi + 533.9\varphi^2\right) \tag{37}$$

where φ is equal to the total volume concentration of each nanoparticle in order to determine the viscosity of the hybrid nanofluid [46].

In addition, the thermophysical properties of the nanoparticles are shown in Table 1.

The friction factor (f) can be calculated using the following expression [51]:

$$f = \frac{\Delta P 2 D_h}{L\rho V^2} \tag{38}$$

Table 1
Thermophysical properties of nanoparticles [47,48,49,50].

Properties	Graphite	TiO_2	MgO	Ag
ρ(kg/m^3)	2210	4250	3560	10,500
C_p(J/kgK)	709	686.2	955	235
k(W/mK)	1950	8.9538	45	429

where ΔP is the pressure drop (Pa), D_h is the hydraulic diameter (m), L is the length (m), and V is the velocity (m/s).

The performance evaluation criterion (PEC) expresses the relationship between the friction factor and the efficiency of the working fluid. It is calculated as follows [51]:

$$PEC = \frac{\frac{Q}{Q_o}}{\left(\frac{f}{f_o}\right)^{1/3}} \tag{39}$$

where subscript o represents the pure water case. Q is the useful heat generation and depends on the temperature difference and specific heat of the heat transfer fluid.

Computational model

ANSYS Fluent 2020 R1 based on the finite volume method is used to solve the Navier-Stokes and energy equations. The radiative transfer equation that consists of absorbing, emitting, and scattering elements is calculated by choosing Discrete Ordinates (DO) method. In the DO method, which is the directional variation of the radiation intensity, the transfer equation is solved by including the total solid angle range of 4π [26]. By integrating the RTE into each wavelength range, the radiation spectrum is divided into the wavelength bands by the DO method. Phi (N_φ) and Theta (N_θ) divisions are implemented to discretise the octane of the angular space and define the control angles. In 2D heat transfer and fluid flow solutions, ANSYS Fluent can only resolve $4N_\theta N_\varphi$ [29]. The SIMPLE algorithm is employed for the pressure–velocity coupling with the second-order upwind differencing scheme for discretization of equations. Least Squares Cell Based and PRESTO! are applied for gradient and discretization of the momentum equations, respectively. The residual values are that the governing equations are set below 10^{-5} while the energy and DO equations are set below 10^{-6} in order to reduce the imbalance of the results. 5x5 Theta and Phi Divisions and 3X3 Theta and Phi Pixels are selected to obtain more accurate and reasonable results [29].

Grid independence test

A non-uniform mesh is generated inside the collector domain, as shown in Fig. 2(a, b). As seen in Fig. 3, different grid numbers are controlled for temperature and velocity using water-based Graphite nanofluid in different volume concentrations by applying mesh numbers of 4000, 16000, 36,000 and 64000.

Model validation

Some previous studies reported in the literature are used to validate the numerical model reported herein. Thus, the work of Otanicar et al. [17], which conducted both experimental and numerical analyses of the direct absorption solar collector, is chosen for the first validation. The nanofluid with mass flow rate of 42 ml/h enters the collector. It receives a sunbeam power density of 1000 W/m^2 and exhibits a combined radiative and convective heat loss of 23 $Wm^{-2}K^{-1}$ due to the glass layer on the top wall. The current collector efficiency as a function of particle concentration matches well with reference study [17] as shown in Fig. 4a. The maximum and average errors of Graphite/water nanofluid are also 11% and 6.02%, respectively. Tyagi et al. [30] performed

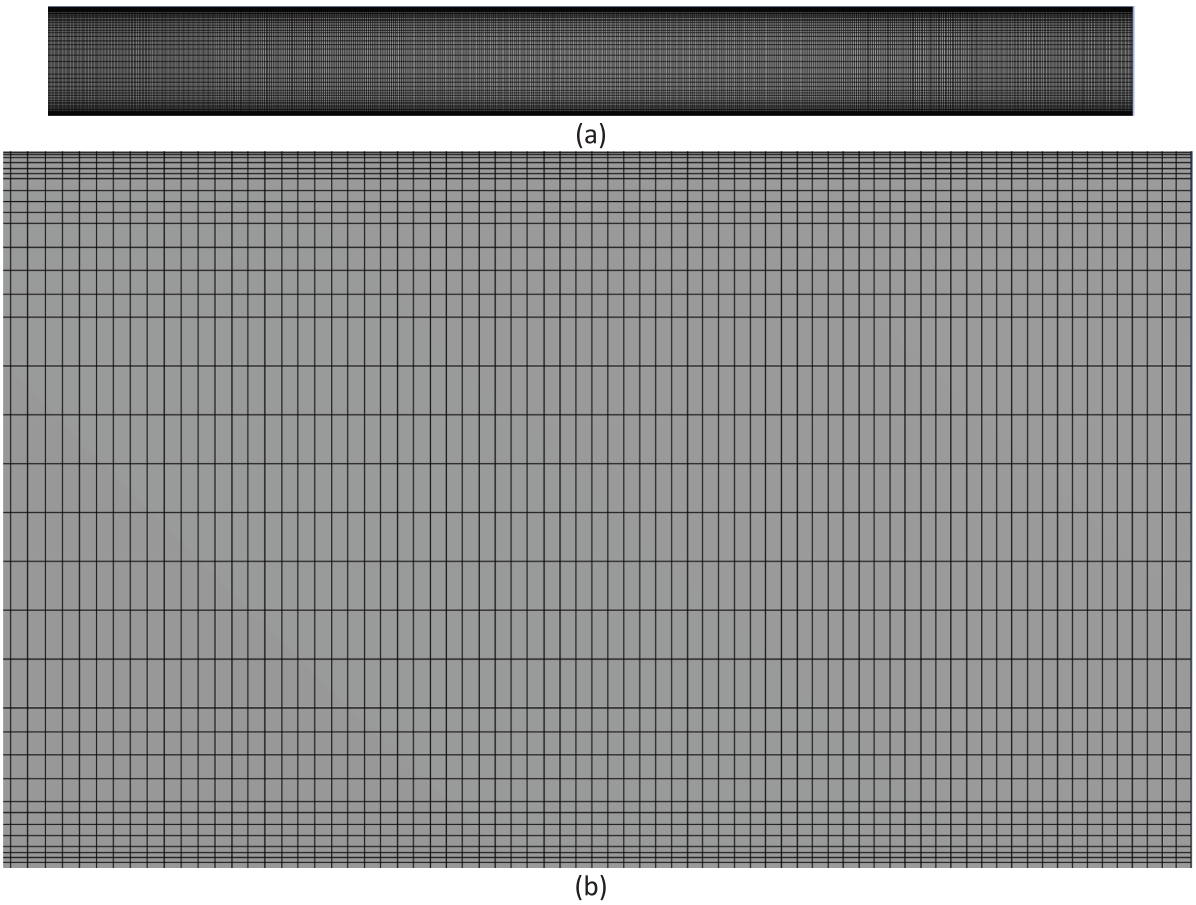

Fig. 2. Mesh distribution along the collector.

numerical analysis of the direct absorption solar collector using water-Al nanofluid and our results are benchmarked with their results in Fig. 4b. The top plate is exposed to an irradiation power density of 1000 W/m^2 while the convective heat loss to the atmosphere from the top wall is 6 $Wm^{-2}K^{-1}$. Fig. 4b compares the current collector efficiency as a function of collector height and is in a good agreement with that reported in the literature [30]. As seen in Fig. 4(b), the maximum and mean errors of the nanofluid are 6.25% and 4.49%, respectively.

Results and discussion

Effect of single nanoparticle on thermal performance

Since different types of nanoparticles have different optical and thermophysical properties, their thermal performances also differ. Fig. 5 shows the performance of different types of mono nanofluids in the collector as a function of volume concentration. The addition of nanoparticles to the base fluid improves the extinction coefficient of the heat transfer fluid. Thus, it increases the capacity of nanofluid to absorb solar energy. As can be seen in Fig. 5a, especially when the volume concentration is 1%, since the temperature gain of nanofluid is higher than that of pure water, the ratio of temperature gain exceeds 1. As the volume concentration of the nanoparticles increases, however, it causes a decrease in the temperature gain of the nanofluid, as shown in Fig. 5. This can be explained that when the volume concentration of the nanoparticles in the fluid is low, sunlight can reach the bottom of the collector such as at 1% or 2%, as seen in Fig. 6. Hence, the temperature of the nanofluid increases more, causing the fluid in the vicinity of the collector base to heat up. The increase in the volume concentration of the nanoparticles ensures that the solar radiation cannot penetrate further into the collector. This reduces the temperature of the nanofluid by allowing more of the radiation to be absorbed by the fluid around the upper wall. It ensures that the temperature differences in the collector are less due to the reduced temperature gain (see Fig. 6).

Furthermore, an increase in the volume concentration provides a decrease in the top wall temperature of the collector. Due to the decreasing temperature, the combined radiation and convection from the glass coating of the collector to the atmosphere causes a decrease in heat loss (see Fig. 5b). Reduced heat losses contribute to the improvement of the thermal performance of the collector, as indicated in Fig. 5c. Moreover, the addition of nanoparticles to the host fluid increases the capacity of the nanofluid to store solar energy while the stored capacity of the pure water is 5.5 W. Therefore, Fig. 5d shows that for solar collector that is volumetrically heated, nanofluid can be used both as a heat transfer fluid and as a storage medium which depends on the initial and final state of the system.

Effect of blended nanoparticle on thermal performance

One of the most important factors affecting photo-thermal conversion efficiency is the type of heat transfer fluid. Increasing the capacity of the fluid to absorb solar energy can improve the conversion performance. Therefore, it can be beneficial to use hybrid nanoparticles instead of mono nanoparticle. In Fig. 5c, since MgO nanoparticles improve the efficiency of the collector more than other nanoparticles incorporated in water, it can be thought that they can also improve their thermal performance when combined with other nanoparticles. Therefore, blended nanoparticles are obtained by combining MgO to Graphite, Ag and TiO_2 nanoparticles and dispersed in water. In the blended mixture formed by adding MgO nanoparticles, temperature gain is

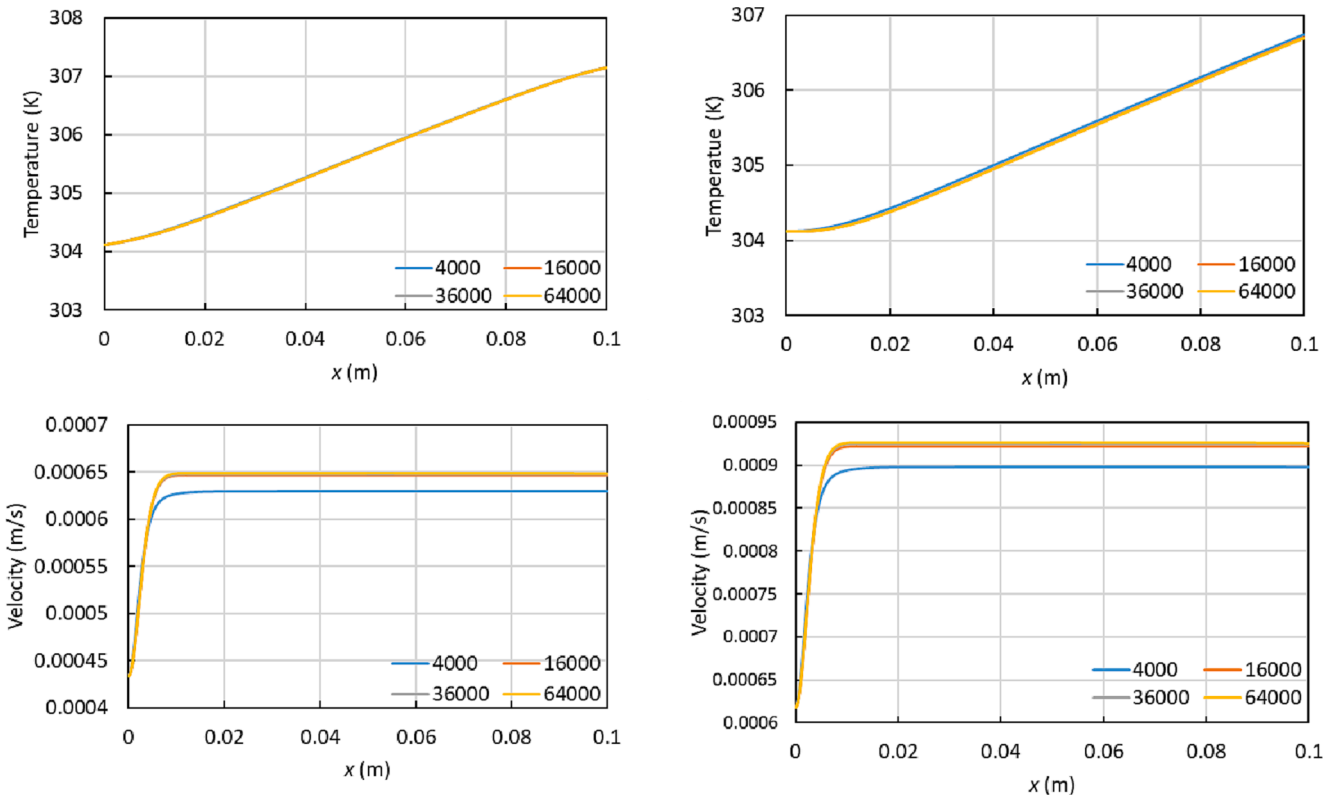

Fig. 3. Variations of temperature and velocity profiles for Graphite/water nanofluid at volume concentrations of 0% (left column) and 1% (right column) with different grid numbers.

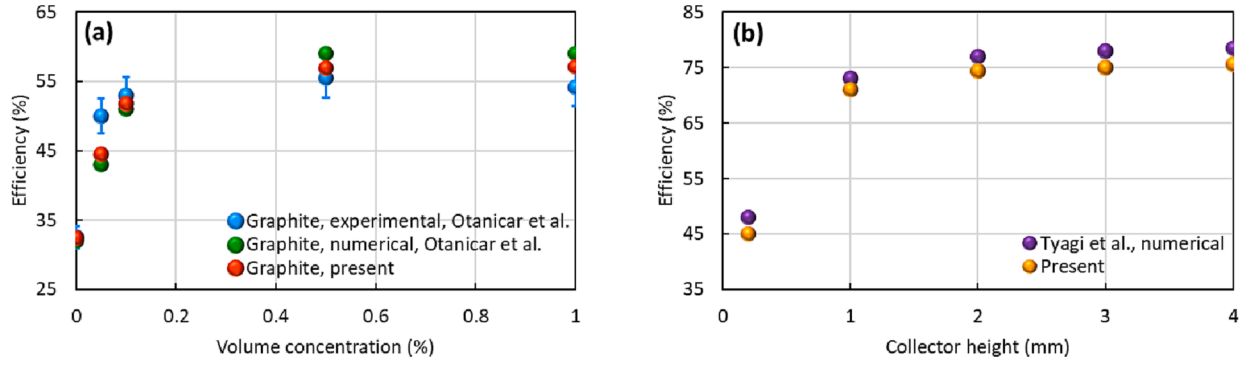

Fig. 4. Comparison of current collector efficiency with that reported in the literature: (a) as a function of volume concentration of particle [17] and (b) as a function of collector height [29].

increased in each hybrid mixture, as shown in Fig. 7a. With the increasing temperature, the heat loss to the environment increases due to the increasing upper wall temperature (see the contour in Fig. 8), as well as the heat loss rate (Fig. 7b). Besides, hybrid nanoparticles not only improve the optical properties of the fluid, but also improve the thermophysical properties. Therefore, the blended particles with enhanced thermal performances allow for the photo-thermal conversion of the collector to be enhanced (Fig. 7c). For example, while the PEC of water/Ag nanofluid is 1.43, it increased to 1.58 with the addition of MgO nanoparticle. Furthermore, the blended particles increase the energy that can be stored as shown in Fig. 7d, by contributing to the enthalpy development in addition to the temperature gain of the fluid.

Moreover, as indicated in Fig. 8, increasing the volume concentration increases the flow rate of the nanofluid, enabling the heat transfer fluid to move faster in the collector. Therefore, the temperature gain of the nanofluid decreases as it is inversely proportional to the volume concentration. Thus, it causes a decrease in the upper wall temperature of the collector.

Because the thermal performances (PEC) of MgO/water and Graphite + MgO/water nanofluids are higher when compared to other types of nanofluids, a comparative analysis of both mono and hybrid nanoparticles would provide a deeper insight into the thermo-fluid behaviour.

Effect of operating temperature on thermal performance

Another factor affecting the photo-thermal conversion efficiency is the fluid temperature. Since the increase or decrease of the fluid temperature causes the thermophysical properties to change, the thermal performance of the collector is also affected. Increasing the inlet temperature of the fluid causes an increase in the collector glass temperature, increasing the heat loss to the atmosphere, which in turn, decreases

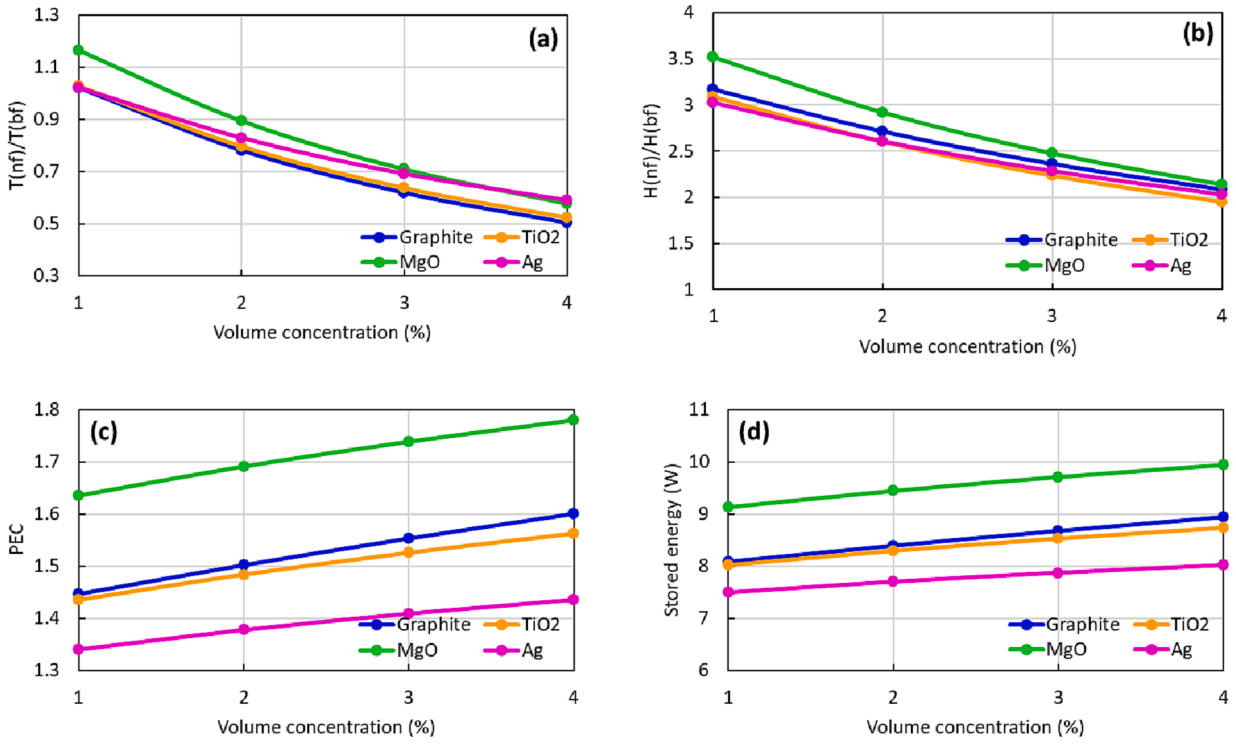

Fig. 5. Effect of water-based mono nanofluids on the thermal performance of the collector: (a) temperature gain rate, (b) heat loss rate, (c) performance evaluation criterion (PEC), and (d) stored energy as a function of volume concentration of the nanofluid.

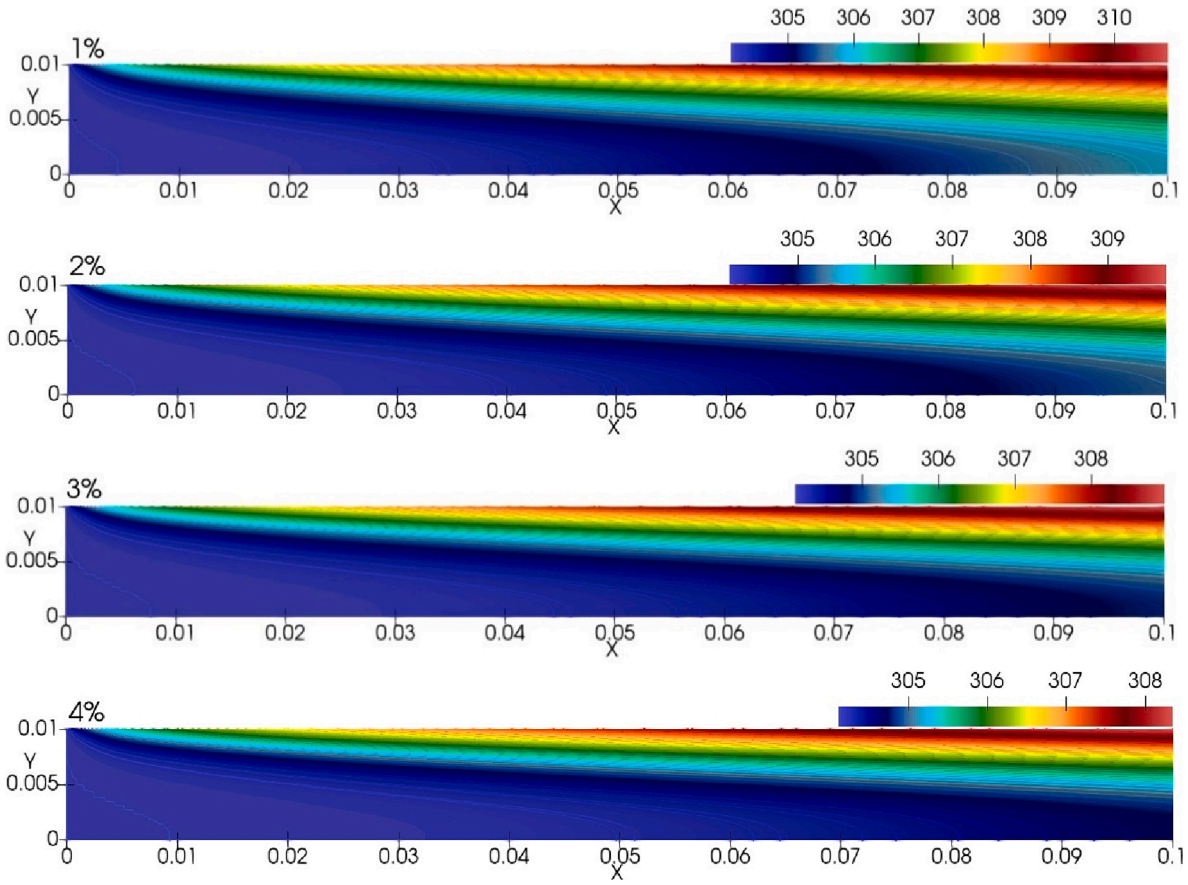

Fig. 6. Temperature (K) contours of TiO_2/water nanofluid at different volume concentrations.

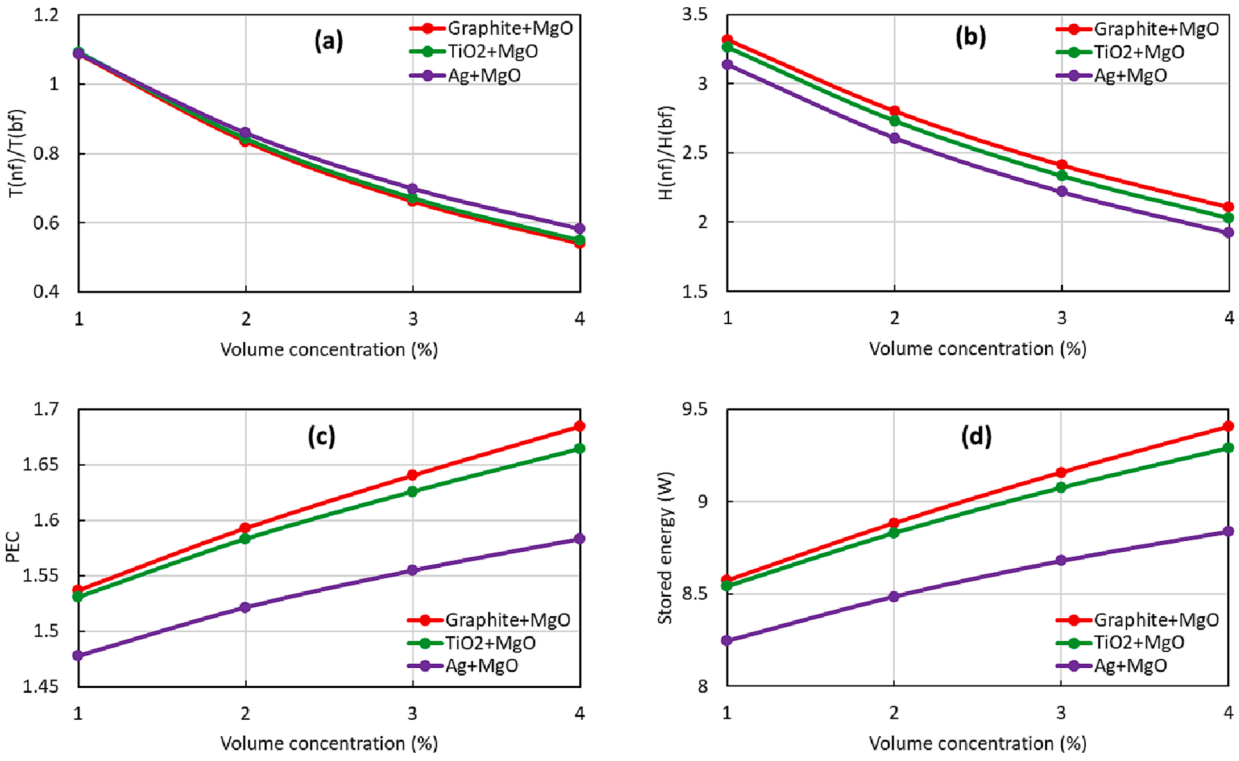

Fig. 7. Effect of water-based hybrid nanofluids on the thermal performance of the collector (a) temperature gain rate, (b) heat loss rate, (c) performance evaluation criterion (PEC), and (d) stored energy rate with changing volume concentrations.

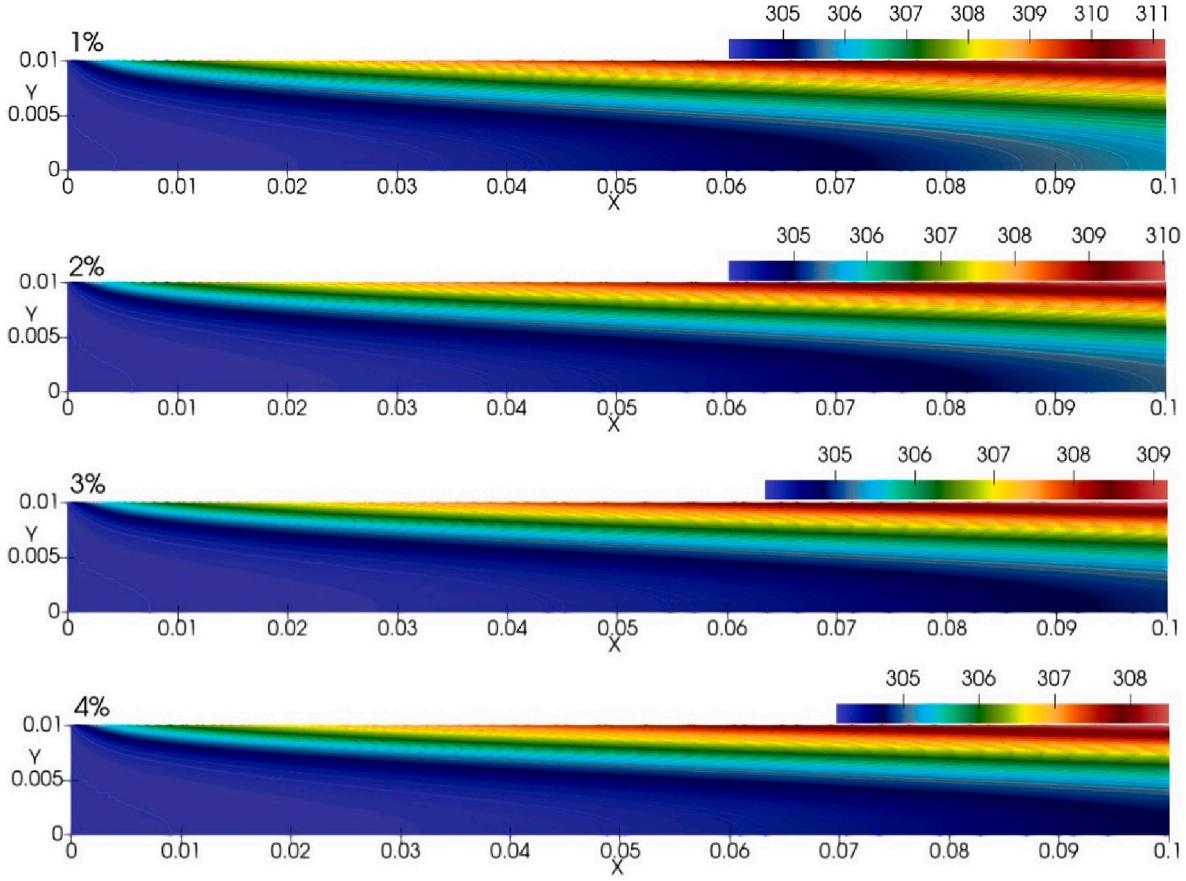

Fig. 8. Temperature (K) contours of TiO_2 + MgO/water nanofluid at different volume concentrations.

the temperature gain of the collector (Figs. 9-10)). But the reason why the temperature gain ratio seems to have increased in Fig. 9a shows the ratio of nanofluid to pure water. For example, the temperature gain ratio of pure water decreases from 2.12 to 1.09, while the temperature gain ratio of MgO/water nanofluid declines from 2.5 to 2.09, and the temperature gain rate is seen to increase from 1.18 to 1.92. Similarly, the heat losses of pure water (from 29 W/m^2 to 495 W/m^2) and MgO/water (from 123 W/m^2 to 609 W/m^2) fluids increase, and the heat loss rate drops from 4.24 to 1.23. Decreased temperature gain ratio and increased heat losses cause the nanofluid to lessen the amount of heat absorbed by solar radiation. The heat gain of pure water decreased from 5.73 to 2.03 while the gain of Graphite + MgO blended nanofluid decreased from 9.05 to 4.89. This drop causes a decrease in both the efficiency of photo-thermal conversion and the stored energy. In Fig. 9(c), however, the increase in the working temperature shows that there is an increase in the PEC. The reason for this is that the graphs show the ratio of nanofluid to pure water. As seen in Fig. 9(d), because the enthalpy change depends on the temperature gain of the heat transfer fluid, the stored energy declines with increasing inlet temperature due to the decreasing the temperature increase of the fluid.

Furthermore, as seen in Fig. 9(c), mono nanofluid performs better than hybrid nanofluid, while in Fig. 9(d) it is seen that they have the same performance at the same volume concentrations. This is because the physical properties of blended nanoparticles are different from mono nanoparticles. Due to the homogeneous of MgO nanoparticles in the hybrid nanoparticle, the increase in the density and thermal conductivity of the blended nanoparticle may be less compared to the MgO/water nanofluid. Because of these situations, such a trend may be obtained.

Effect of collector length on thermal performance

The effect of collector length on the energy conversion performance is shown in Fig. 11. An increase in the collector length means an increase in the length of the glass plate of the collector. This increasing length boosts the amount of solar radiation penetrating per unit area, increasing the temperature of the heat transfer fluid. While the temperature increase ratio of pure water rises from 3.1 to 11.1 with increasing collector length, the temperature of Graphite + MgO/water nanofluid increases from 3.4 to 10.9 at volume concentration of 1%, and the enhancement rate of nanofluid to pure water is 1.1 and 0.98 for 0.1 m and 0.35 m lengths, respectively (Fig. 11a). As shown in Fig. 12, the temperature enhancement of the fluid causes an increase in the top wall temperature of the collector, causing an increase in the heat loss to the environment. While the combined radiation and convection heat loss of pure water increases with the collector length from 40.9 W/m^2 to 141.2 W/m^2, the heat loss of MgO/water nanofluid increases from 141.9 W/m^2 to 252.7 W/m^2, and the heat loss ratios of nanofluid to pure water become 3.5 and 1.79 (Fig. 11b), respectively. The increase in heat loss negatively affects the photo-thermal conversion of the collector, resulting in a decrease in the thermal performance of the collector (Fig. 11(c)). As the collector length increases, on the other hand, the fluid's outlet temperature increases that the stored capacity of the fluid enhances (Fig. 11(d)).

Conclusions

Herein, the photo-thermal conversion performance of volumetrically heated solar collector with mono-nanoparticle and hybrid-nanoparticle filled fluids desired for a direct solar energy system was numerically investigated. By solving 2D radiation heat transfer and energy equations with ANSYS Fluent, the effects of collector length, operating temperature, and volume concentration of nanoparticle on the photo-thermal conversion efficiency, are analysed. The addition of nanoparticles to pure water increased the extinction coefficient of the nanofluid and increased its solar energy absorption capacity. This increase was improved by increasing the volume concentration of the particles and the addition of blended particles. Besides, the increase in the volume concentration decreased the penetration of sunlight with the increase in depth of the collector, and most of the sunlight was absorbed by the

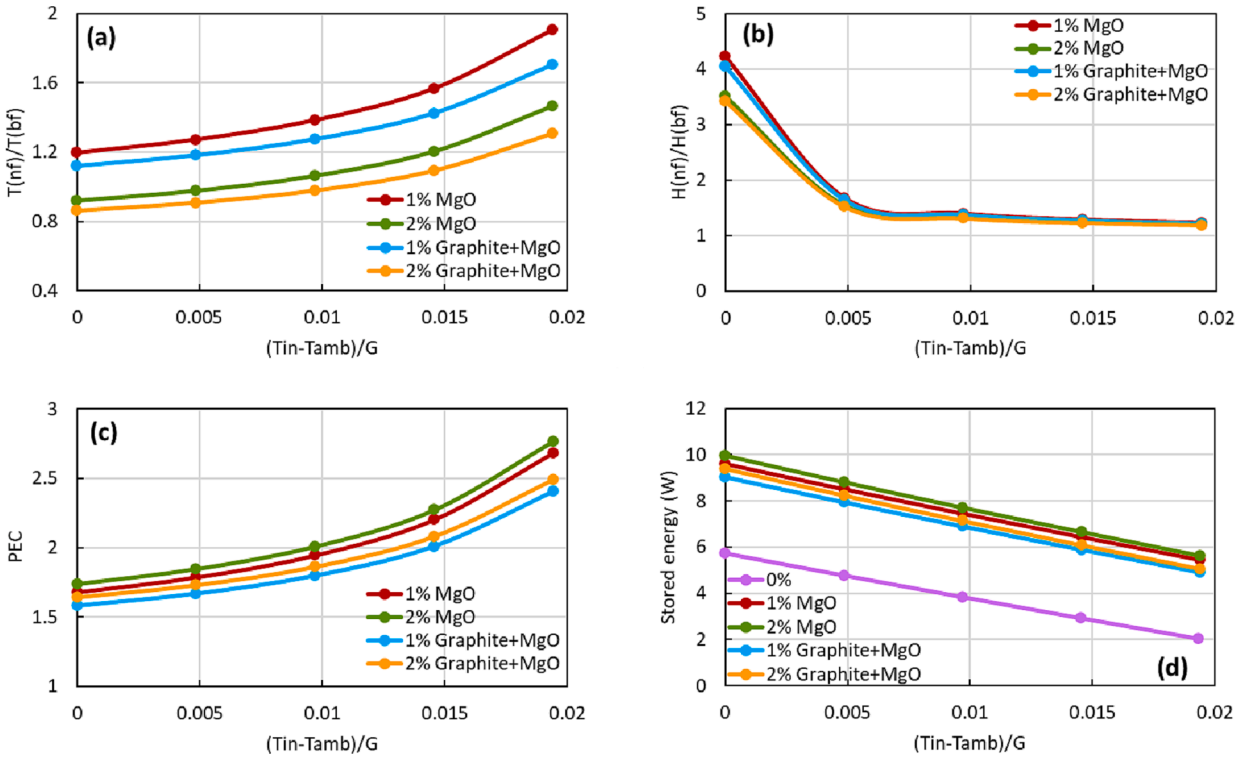

Fig. 9. Effect of working temperature on the thermal performance of the collector (a) temperature gain rate, (b) heat loss rate, (c) performance evaluation criterion (PEC), and (d) stored energy rate with changing inlet temperatures.

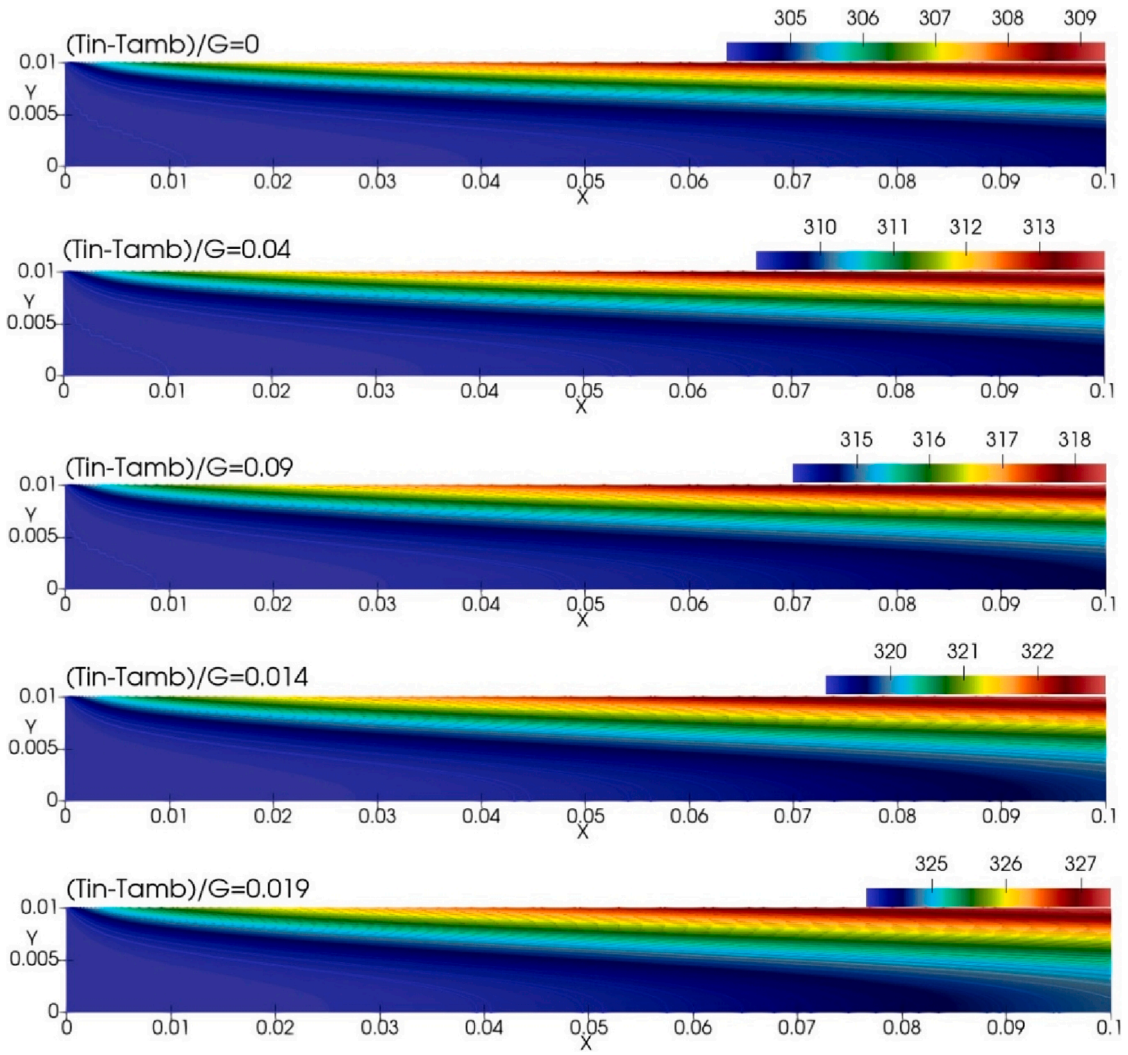

Fig. 10. Temperature (K) contours of Graphite + MgO nanofluid at different inlet temperatures.

nanofluid at the vicinity of the top wall. Increasing volume concentration caused a decrease in temperature differences in the collector. Furthermore, the increase in the working temperature of the fluid increased the heat transfer to the environment by increasing the temperature of the collector. This has caused a decline in the useful heat production of the collector from the solar energy. The increase in collector length also negatively affected the photo-thermal conversion performance. With increasing collector length, the increase in the amount of solar energy absorption of the nanofluid caused an increase in the top wall temperature of the collector, increasing the heat losses. Moreover, the use of hybrid particles was demonstrated the usability of hybrid nanofluids in solar energy applications by increasing the sensible energy storage.

To sum up, the significance of the current research is to physically examine the factors affecting the photo-thermal conversion performance of volumetrically heated nanofluids in order to filling the research gaps as demonstrated in the literature review. This work clearly illustrates that the maximum PEC and sensible heat are obtained when the volume concentration is 4%. The maximum performance evaluation criterion (PEC) is also obtained in the case of operating temperature $\left(\frac{T_{in}-T_{amb}}{G}\right)$ and collector length of 0.19 m and 0.1 m, respectively, while the maximum sensible heat can be found in the case of 0 and 0.35 m. When the volume concentration of the Graphite + MgO/water nanofluid is improved from 1% to 4%, the average PEC and sensible heat storage are 1.62 W and 9.01 W, respectively. As the operating temperature augments from 0 to 0.019, the average PEC and sensible heat storage are 1.96 W and 7.19 W, respectively. When the collector length increases from 0.1 m to 0.35 m, the average PEC and sensible heat storage are 1.57 W and 48.7 W, respectively. Finally, the utilisation of phase change materials in volumetrically heated solar collectors remains a future scope.

CRediT authorship contribution statement

Oguzhan Kazaz: Conceptualization, Methodology, Software, Validation, Investigation, Formal analysis, Visualization, Writing – original draft, Writing – review & editing. **Nader Karimi:** Conceptualization, Supervision, Writing – review & editing. **Shanmugam Kumar:** Supervision, Writing – review & editing. **Gioia Falcone:** Supervision, Writing – review & editing. **Manosh C. Paul:** Conceptualization, Supervision, Writing – review & editing, Project administration, Resources, Funding acquisition.

Declaration of Competing Interest

The authors declare that they have no known competing financial interests or personal relationships that could have appeared to influence the work reported in this paper.

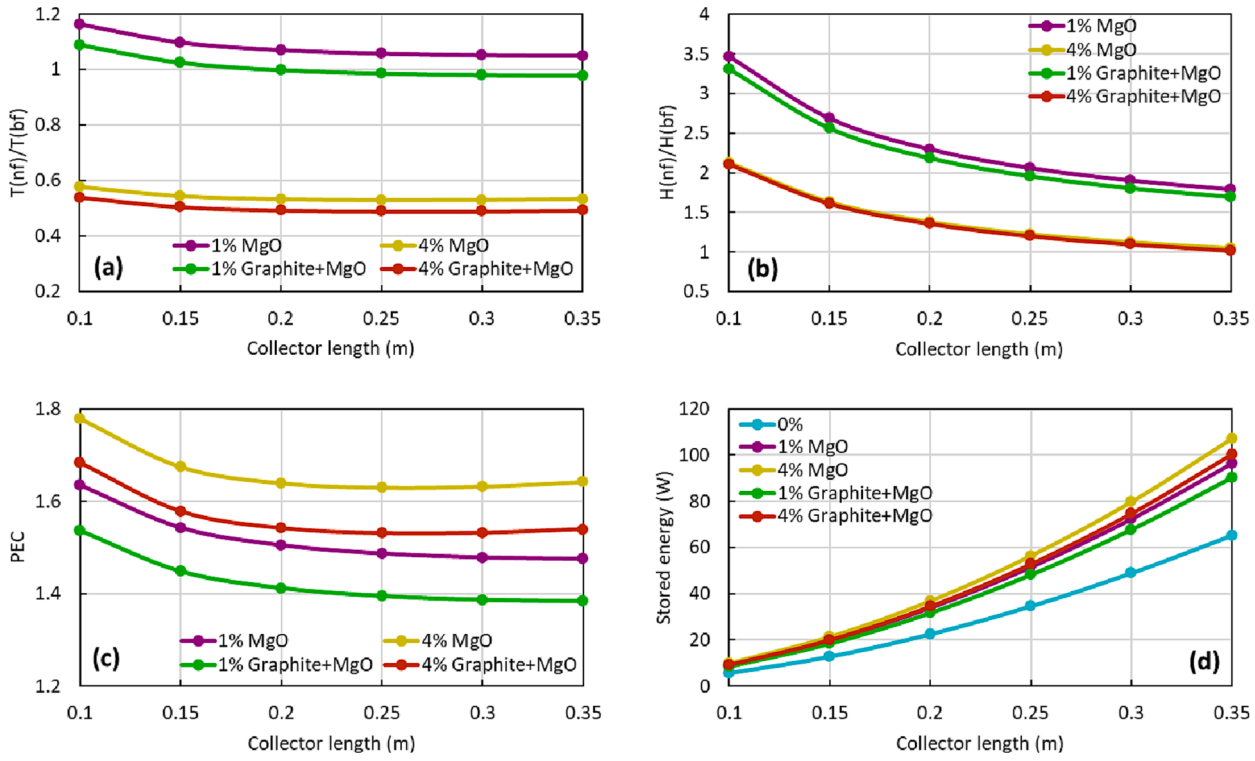

Fig. 11. Effect of collector length on thermal performance of the collector (a) temperature gain rate, (b) heat loss rate, (c) performance evaluation criterion (PEC), and (d) stored energy rate with changing collector distance.

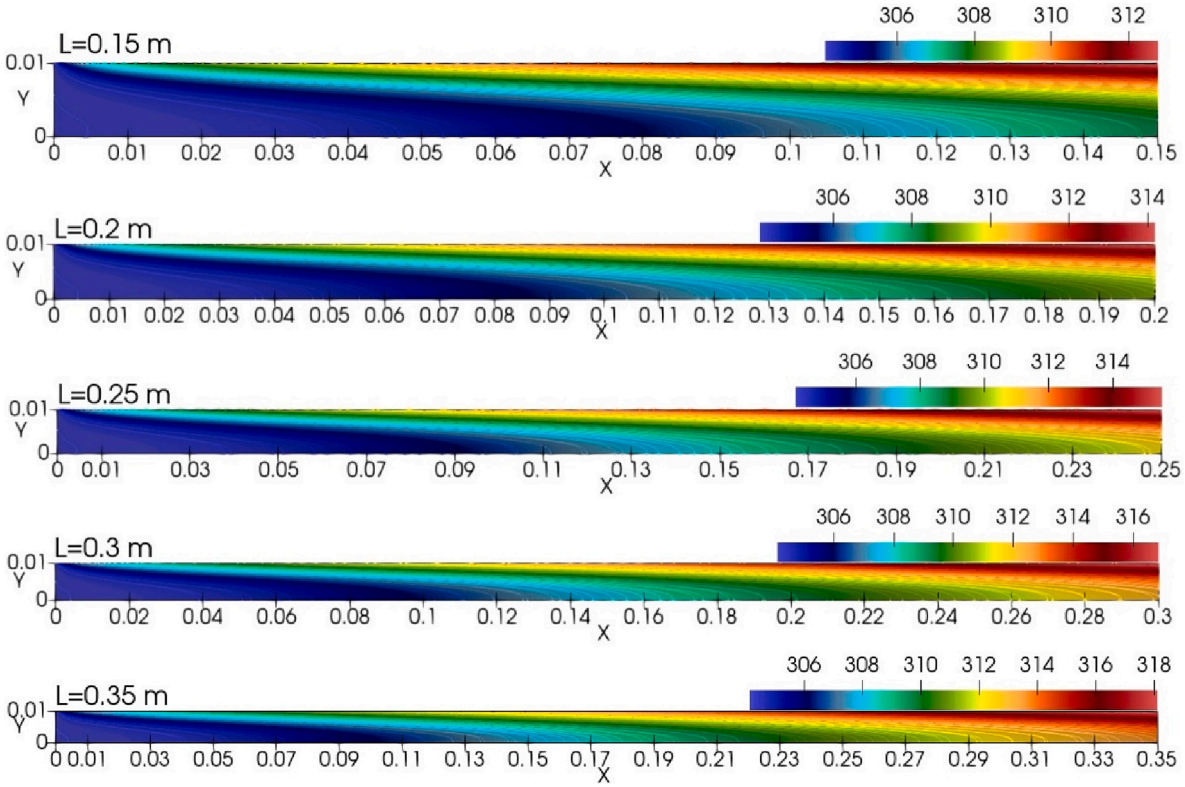

Fig. 12. Temperature (K) contours of Graphite + MgO nanofluid at different collector lengths.

Data availability

The data that support the findings of this study are available from the corresponding author upon reasonable request.

Acknowledgments

The first author would like to thank the Turkish Ministry of National Education, Republic of Turkey for funding his PhD research study at the University of Glasgow. Preliminary results of the paper were presented in the 17th UK Heat Transfer Conference, Manchester, UK, 03-05 April 2022 [52].

References

[1] A. Arsalis, A comprehensive review of fuel cell-based micro-combined-heat-and-power systems, Renew. Sustain. Energy Rev. 105 (2019) 391–414.
[2] I. Khan, F. Hou, A. Zakari, V.K. Tawiah, The dynamic links among energy transitions, energy consumption, and sustainable economic growth: A novel framework for IEA countries, Energy 222 (2021), 119935.
[3] M.A. Bagherian, K. Mehranzamir, A comprehensive review on renewable energy integration for combined heat and power production, Energ. Conver. Manage. 224 (2020), 113454.
[4] J.C. Alberizzi, J.M. Frigola, M. Rossi, M. Renzi, Optimal sizing of a Hybrid Renewable Energy System: Importance of data selection with highly variable renewable energy sources, Energ. Conver. Manage. 223 (2020), 113303.
[5] B.M. Opeyemi, Path to sustainable energy consumption: The possibility of substituting renewable energy for non-renewable energy, Energy 228 (2021), 120519.
[6] M. Shahbaz, B.A. Topcu, S.S. Sarıgül, X.V. Vo, The effect of financial development on renewable energy demand: The case of developing countries, Renew. Energy 178 (2021) 1370–1380.
[7] V. Khullar, H. Tyagi, N. Hordy, T.P. Otanicar, Y. Hewakuruppu, P. Modi, R. A. Taylor, Harvesting solar thermal energy through nanofluid-based volumetric absorption systems, Int. J. Heat Mass Transf. 77 (2014) 377–384.
[8] E.P.B. Filho, O.S.H. Mendoza, C.L.L. Beicker, A. Menezes, D. Wen, Experimental investigation of a silver nanoparticle-based direct absorption solar thermal system, Energ. Conver. Manage. 84 (2014) 261–267.
[9] J. Qu, M. Tian, X. Han, R. Zhang, Q. Wang, Photo-thermal conversion characteristics of MWCNT-H2O nanofluids for direct solar thermal energy absorption applications, Appl. Therm. Eng. 124 (2017) 486–493.
[10] K. Wang, Y. He, Z. Zheng, J. Gao, A. Kan, H. Xie, W. Yu, Experimental optimization of nanofluids based direct absorption solar collector by optical boundary conditions, Appl. Therm. Eng. 182 (2021), 116076.
[11] C. Guo, C. Liu, S. Jiao, R. Wang, Z. Rao, Introducing optical fiber as internal light source into direct absorption solar collector for enhancing photo-thermal conversion performance of MWCNT-H2O nanofluids, Appl. Therm. Eng. 173 (2020), 115207.
[12] R.C. Shende, S. Ramaprabhu, Thermo-optical properties of partially unzipped multiwalled carbon nanotubes dispersed nanofluids for direct absorption solar thermal energy systems, Sol. Energy Mater. Sol. Cells 157 (2016) 117–125.
[13] M. Valizade, M.M. Heyhat, M. Maerefat, Experimental comparison of optical properties of nanofluid and metal foam for using in direct absorption solar collectors, Sol. Energy Mater. Sol. Cells 195 (2019) 71–80.
[14] M. Hatami, D. Jing, Evaluation of wavy direct absorption solar collector (DASC) performance using different nanofluids, J. Mol. Liq. 229 (2017) 203–211.
[15] M. Chen, Y. He, J. Zhu, Y. Shuai, B. Jiang, Y. Huang, An experimental investigation on sunlight absorption characteristics of silver nanofluids, Sol. Energy 115 (2015) 85–94.
[16] T.B. Gorji, A.A. Ranjbar, A numerical and experimental investigation on the performance of a low-flux direct absorption solar collector (DASC) using graphite, magnetite and silver nanofluids, Sol. Energy 135 (2016) 493–505.
[17] T.P. Otanicar, P.E. Phelan, R.S. Prasher, G. Rosengarten, R.A. Taylor, Nanofluid-based direct absorption solar collector, J. Renewable Sustainable Energy 2 (3) (2010) 033102–033113.
[18] T.B. Gorji, A.A. Ranjbar, Thermal and exergy optimization of a nanofluid-based direct absorption solar collector, Renew. Energy 106 (2017) 274–287.
[19] Z. Luo, C. Wang, W. Wei, G. Xiao, M. Ni, Performance improvement of a nanofluid solar collector based on direct absorption collection (DAC) concepts, Int. J. Heat Mass Transf. 75 (2014) 262–271.
[20] S.K. Verma, A.K. Tiwari, S. Tiwari, D.S. Chauhan, Performance analysis of hybrid nanofluids in flat plate solar collector as an advanced working fluid, Sol. Energy 167 (2018) 231–241.
[21] A.A. Minea, W.M. El-Maghlany, Influence of hybrid nanofluids on the performance of parabolic trough collectors in solar thermal systems: Recent findings and numerical comparison, Renew. Energy 120 (2018) 350–364.
[22] O.A. Hussein, K. Habib, A.S. Muhsan, R. Saidur, O.A. Alawi, T.K. Ibrahim, Thermal performance enhancement of a flat plate solar collector using hybrid nanofluid, Sol. Energy 204 (2020) 208–222.
[23] R. Ekiciler, K. Arslan, O. Turgut, B. Kurşun, Effect of hybrid nanofluid on heat transfer performance of parabolic trough solar collector receiver, J. Therm. Anal. Calorim. 143 (2021) 1637–1654.
[24] A. Joseph, S. Sreekumar, C.S. Sujith Kumar, S. Thomas, Optimisation of thermo-optical properties of SiO2/Ag–CuO nanofluid for direct absorption solar collectors, J. Mol. Liq. 296 (2019), 111986.
[25] M. Karami, Experimental investigation of first and second laws in a direct absorption solar collector using hybrid Fe3O4/SiO2 nanofluid, J. Therm. Anal. Calorim. 136 (2019) 661–671.
[26] M.F. Modest, Radiative Heat Transfer, Academic Press, 2013.
[27] O. Kazaz, N. Karimi, S. Kumar, G. Falcone, M.C. Paul, Enhanced sensible heat storage capacity of nanofluids by improving the photothermal conversion performance with direct radiative absorption of solar energy, J. Mol. Liq. 372 (2023), 121182.
[28] P. Raj, S. Subudhi, A review of studies using nanofluids in flat-plate and direct absorption solar collectors, Renew. Sustain. Energy Rev. 84 (2018) 54–74.
[29] ANSYS Fluent User's Guide, Canonsburg: ANSYS, Inc., 2013.
[30] H. Tyagi, P. Phelan, R. Prasher, Predicted Efficiency of a Low-Temperature Nanofluid-Based Direct Absorption Solar Collector, J. Sol. Energy Eng. 131 (4) (2009), 041004.
[31] T.B. Gorji, A.A. Ranjbar, A review on optical properties and application of nanofluids in direct, Renew. Sustain. Energy Rev. 72 (2017) 10–32.
[32] C.F. Bohren, D.R. Huffman, Absorption and Scattering of Light by Small Particles, Wiley, New York, 1983.
[33] G.M. Hale, M.R. Querry, Optical Constants of Water in the 200-nm to 200-μm Wavelength Region, Appl. Opt. 12 (3) (1973) 555–563.
[34] S. Babar, J.H. Weaver, Optical constants of Cu, Ag, and Au revisited, Appl. Opt. 54 (3) (2015) 477–481.
[35] E.D. Palik, Handbook of Optical Constants of Solids, Academic Press, 1997.
[36] H.M.F. Rabbi, A.Z. Sahin, B.S. Yilbas, A. Al-Sharafi, Methods for the Determination of Nanofluid Optical Properties: A Review, Int. J. Thermophys. 42 (9) (2021) 1–42.
[37] M. Du, G.H. Tang, Plasmonic nanofluids based on gold nanorods/nanoellipsoids/nanosheets for solar energy harvesting, Sol. Energy 137 (2019) 393–400.
[38] C.V. Vital, S. Farooq, E.R. de Araujo, D. Rativa, L.A. Gómez-Malagón, Numerical assessment of transition metal nitrides nanofluids for improved performance of direct absorption solar collectors, Appl. Therm. Eng. 190 (2021), 116799.
[39] J.A. Duffie, W.A. Beckman, Solar Engineering of Thermal Processes, John Wiley & Sons Inc, Hoboken, New Jersey, 2013.
[40] T. Basak, A.J. Chamkha, Heatline analysis on natural convection for nanofluids confined within square cavities with various thermal boundary conditions, Int. J. Heat Mass Transf. 55 (21–22) (2012) 5526–5543.
[41] R.S.R. Gorla, S. Siddiqa, M.A. Mansour, A.M. Rashad, T. Salah, Heat Source/Sink Effects on a Hybrid Nanofluid-Filled Porous Cavity, J. Thermophys Heat Transfer 31 (4) (2017) 847–857.
[42] R.L. Hamilton, O.K. Crosser, Thermal Conductivity of Heterogeneous Two-Component Systems, Ind. Eng. Chem. Fundam. 1 (3) (1962) 187–191.
[43] S.S.U. Devi, S.P. Anjali Devi, Numerical investigation of three-dimensional hybrid Cu–Al2O3/water nanofluid flow over a stretching sheet with effecting Lorentz force subject to Newtonian heating, Can. J. Phys. 94 (5) (2016) 490–496.
[44] Y. Xuan, Q. Li, W. Hu, Aggregation Structure and Thermal Conductivity of Nanofluids, AIChE J 49 (4) (2003) 1038–1043.
[45] B.C. Pak, Y.I. Cho, Hydrodynamic and heat transfer study of dispersed fluids with submicron metallic oxide particles, Exp. Heat Transfer 11 (2) (1998) 151–170.
[46] R.R. Sahoo, J. Sarkar, Heat transfer performance characteristics of hybrid nanofluids as coolant in louvered fin automotive radiator, Heat Mass Transf. 53 (2017) 1923–1931.
[47] Y.A. Cengel, B.S. Klein, Heat Transfer: A Practical Approach, WBC McGraw-Hill, Boston, 1998.
[48] B. Ghasemi, S.M. Aminossadati, Periodic natural convection in a nanofluid-filled enclosure with oscillating heat flux, Int. J. Therm. Sci. 49 (1) (2010) 1–9.
[49] R. Davarnejad, M. Jamshidzadeh, CFD modeling of heat transfer performance of MgO-water nanofluid under turbulent flow, Eng. Sci. Technol., Int. J. 18 (4) (2015) 536–542.
[50] M. Sheikholeslami, D.D. Ganji, H.R. Ashorynejad, Investigation of squeezing unsteady nanofluid flow using ADM, Powder Technol. 239 (2013) 259–265.
[51] E. Bellos, C. Tzivanidis, D. Tsimpoukis, Enhancing the performance of parabolic trough collectors using nanofluids and turbulators, Renew. Sustain. Energy Rev. 91 (2018) 358–375.
[52] O. Kazaz, N. Karimi, S. Kumar, M. C. Paul and G. Falcone, "Effects of Combined Radiation and Forced Convection on a Directly Capturing Solar Energy System," in *17th UK Heat Transfer Conference (UKHTC2021)*, Manchester, 2022.